

## Scattering of 18.7-Mev Alpha Particles from Al, Cu, and Ag†

O. H. GAILLAR,\* E. BLEULER, AND D. J. TENDAM  
*Department of Physics, Purdue University, Lafayette, Indiana*

(Received August 28, 1958)

The scattering of 18.7-Mev alpha particles from Ag, Cu, and Al was studied from  $10^\circ$  to  $170^\circ$  with rms angular resolutions of  $0.4^\circ$  to  $0.85^\circ$ . The scattered alpha particles were separated from singly charged reaction products with the aid of a proportional counter, and their energies were measured with a CsI(Tl) scintillation spectrometer. The elastic scattering for Ag shows the "exponential" dropoff from the Coulomb cross section, without any pronounced structure at large angles. For Cu, definite changes in the slope of the dropoff are observed up to  $120^\circ$ , followed by a shallow minimum near  $130^\circ$  and a very deep, narrow minimum at  $162^\circ$  (c.m.). The interaction radii deduced from the strong-absorption model agree with those found at higher energies. From the diffraction-like pattern found for Al, an interaction radius of  $6.4 \times 10^{-13}$  cm is derived, appreciably larger than the one obtained at 40 Mev ( $5.4 \times 10^{-13}$  cm). There are indications that a direct-process interpretation of the inelastic scattering from Al is possible.

### I. INTRODUCTION

THE reasons for the renewed interest in alpha-particle scattering are discussed by Seidlitz, Bleuler, and Tendam<sup>1</sup> and need not be repeated here. After the preliminary measurements of the scattering of 19-Mev alpha particles from Al and Cu performed by Bleuler and Tendam,<sup>2</sup> a more thorough study of the scattering of alpha particles by light nuclei was started in this laboratory. Seidlitz *et al.*<sup>1</sup> used gas targets (Ne, A) and photographic-plate registration whereas the present work, done concurrently, employed metal-foil targets (Al, Cu, Ag) with electronic detection techniques. Emphasis was laid on good geometry (rms angular width  $< 0.5^\circ$ ) and a large range of angles ( $10^\circ$  to  $170^\circ$ ), scanned in small steps ( $2^\circ$  or less). The smallness of the steps and the extension of the range of scattering angles to the far backward direction were prompted largely by the narrow oscillations of the cross section for elastic scattering and its rise at large angles obtained in the strong-absorption theories.<sup>3,4</sup>

### II. EXPERIMENTAL METHOD AND TECHNIQUE

The alpha-particle beam is brought out of the cyclotron room and focused by a pair of quadrupole magnets. It then enters a scattering chamber and is scattered by various foils. The scattered particles are detected in a detection head whose position can be varied continuously from  $10^\circ$  to  $170^\circ$ . Reaction products are separated electronically, and the energy of the scattered alpha particles is recorded with the help of a multichannel analyzer.

#### Scattering Chamber

The 18-inch scattering chamber described by Seidlitz, Bleuler, and Tendam<sup>1</sup> was modified and used for this work. A cross section of the chamber is shown in Fig. 1.

† Work supported in part by the U. S. Atomic Energy Commission. This article is based on a doctoral thesis submitted by O. H. Gailar to the faculty of Purdue University.

\* Now at Combustion Engineering, Inc., Windsor, Connecticut.

<sup>1</sup> Seidlitz, Bleuler, and Tendam, *Phys. Rev.* **110**, 682 (1958).

<sup>2</sup> E. Bleuler and D. J. Tendam, *Phys. Rev.* **99**, 1605 (1955).

<sup>3</sup> J. S. Blair, *Phys. Rev.* **95**, 1218 (1954).

<sup>4</sup> Wall, Rees, and Ford, *Phys. Rev.* **97**, 726 (1955).

#### Beam Collimation

The defining apertures of the collimator limit the maximum divergence of the beam to  $\pm 0.5^\circ$ . An insulated probe, *P*, can be inserted behind the first diaphragm to aid in maximizing the beam entering the collimator. The chamber is then aligned with the beam direction by rotations about a vertical and a horizontal axis in the vicinity of the collimator entrance aperture.

#### Foil Ladder

Four different scattering foils are positioned in a "foil ladder" at the center of the chamber. The ladder may be raised or lowered to bring the various scattering foils into the path of the beam without breaking the vacuum. Foils of Al, Cu, Ag, and Au with a nominal thickness of 0.0001 inch were used. The Au foil was included for alignment and control purposes.

#### Beam Measurement

The beam passing through the targets is collected in a Faraday cup of 18-inch depth. The large depth was chosen in order to reduce the background at the counting head produced when the beam strikes the collector, and to minimize the escape of secondary electrons. The latter is further reduced by a transverse magnetic field near the entrance to the collector, produced by a set of permanent magnets. The collected charge is

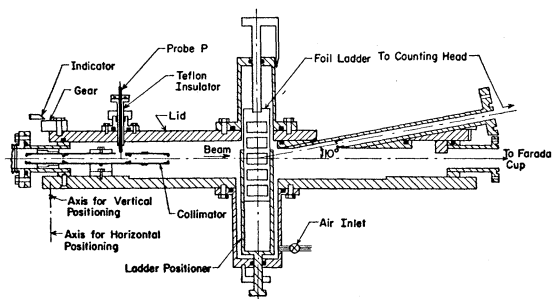


FIG. 1. Scattering chamber.

measured with a current integrator patterned after the one described by Higinbotham and Rankowitz.<sup>5</sup>

The energy of the alpha particles entering the scattering chamber was determined by measuring its mean range in Al.<sup>6</sup>

### Monitors

Two holes at approximately  $\pm 18^\circ$  to the direction defined by the collimator were bored through the wall of the chamber. A monitor consisting of a scintillation crystal and a photomultiplier was placed behind each hole. These monitors were carefully adjusted to make equal angles with the direction defined by the collimator. They were used to align the scattering chamber with the focused beam (within the small angular divergence permitted by the collimator) and to give a check on the beam current as measured by the Faraday cup.

### Rotating Lid

The scattered particles or reaction products reach the detector through a brass tube which passes at an angle of  $10^\circ$  through the lid. In order to vary the scattering angle the lid was rotated, guided by a brass ring soldered to it and bearing against the chamber wall. It was necessary, unfortunately, to let the chamber down to atmospheric pressure each time the scattering angle was changed. Suitable gate valves and by-pass systems were arranged so that the chamber could be re-evacuated in from 15 to 20 minutes. Future work will be done using a ball-bearing race, and it will not be necessary to break the vacuum.

### Detection Head

The detection head consists essentially of a thin proportional ( $dE/dx$ ) counter and a scintillation crystal ( $E$ ) counter. Figure 2 shows a cross section of this detector. The scattered particles pass from the vacuum of the scattering chamber through a Mylar or Al window into the gas of the proportional counter. They traverse the latter lengthwise, losing a fraction of their energy. They then pass through the defining aperture ( $\frac{1}{8}$ - or  $\frac{3}{16}$ -inch diameter) and are stopped in the NaI or CsI scintillator. Limiting diaphragms between the defining aperture and the target allow the crystal to see the entire beam spot on the scattering foil, but not the foil holder. The proportional counter contains a mixture of  $\text{CH}_4$  and either argon or helium at atmospheric pressure, under continuous flow.

### Electronic Technique

A usual fast-slow coincidence arrangement was constructed similar to the one described by Blue and Bleuler.<sup>7</sup>

<sup>5</sup> W. A. Higinbotham and S. Rankowitz, *Rev. Sci. Instr.* **22**, 688 (1951).

<sup>6</sup> Gailar, Seidlitz, Bleuler, and Tendam, *Rev. Sci. Instr.* **24**, 126 (1953).

<sup>7</sup> J. W. Blue and E. Bleuler, *Phys. Rev.* **100**, 1324 (1955).

The  $E$  and  $dE/dx$  pulses were amplified by fast (25 Mc/sec) amplifiers and a fast coincidence (resolving time approximately 40  $\mu\text{sec}$ ) was made between them. This insured that the particle being counted passed through both counters, and came from the correct direction. The  $E$  and  $dE/dx$  pulses were also amplified by linear amplifiers, the amplified  $E$  pulse going to a 20-channel analyzer, the  $dE/dx$  pulse to a single-channel analyzer. The output of the single-channel analyzer made a slow coincidence with the output of the fast coincidence circuit; the resulting coincidence pulse was suitably shaped and used to trigger the 20-channel analyzer.

## III. PRELIMINARY MEASUREMENTS AND CALCULATIONS

### Separation of Particles

The proportional counter is used to distinguish the elastically and inelastically scattered alpha particles from reaction products —  $\text{He}^3$ ,  $\text{H}^3$ ,  $\text{H}^2$ ,  $\text{H}^1$ . Since the ( $\alpha, \text{He}^3$ ) reactions with Al and Cu are endoergic by more than 12 Mev, and only inelastic scattering with energy loss of 1–2 Mev was investigated, no discrimination against  $\text{He}^3$  was necessary. The ( $\alpha, t$ ) and ( $\alpha, d$ ) reactions have  $Q$  values of about –10 Mev, whereas those of the ( $\alpha, p$ ) reactions are of the order of –2 Mev. The chief reaction products to be eliminated are protons and possibly, at large angles, deuterons.

The discrimination is made easy by the fact that the rate of energy loss of an alpha particle is four times larger than that of a singly charged particle of the same velocity. For an argon-filled counter one estimates, using a mean excitation potential of 200 ev, that the ionization produced by an alpha particle with energy less than 19 Mev is larger than that produced by protons of energy above about 0.5 Mev or deuterons of energy above 1 Mev. The pulse height produced by the latter in the scintillation counter corresponds to that of an alpha particle of less than 3 Mev.<sup>8</sup> In principle, then, if only those events are accepted in which the pulse in the proportional counter is larger than that due to a

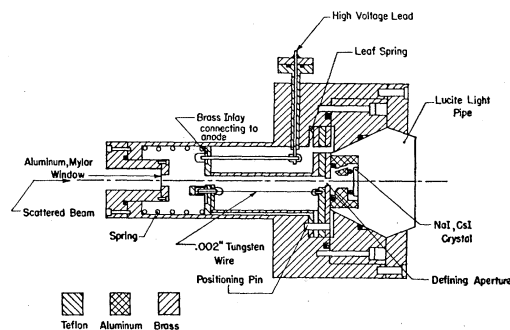


FIG. 2. Detection head; proportional-counter, scintillation-counter telescope.

<sup>8</sup> F. S. Eby and W. K. Jentschke, *Phys. Rev.* **96**, 911 (1954).

19-Mev alpha particle, one is sure that the scintillation detector counts exclusively alpha particles, provided the pulse height corresponds to an alpha energy between 3 and 19 Mev. In practice, the acceptable energy interval is appreciably less because of the straggling of both the proportional-counter and the scintillation-counter response and because of the finite amount of energy lost by the alpha particles in the proportional counter and in the gas space between the two counters.

### Calibration of $dE/dx$ vs $E$ Pulses for Alpha Particles

Since the energy of the scattered alpha particles depends on the particular scattering foil (loss of energy due to ionization) and on the scattering angle (transfer of energy during the collision), the  $dE/dx$  and  $E$  pulse heights changed from one scatterer to another, and from one angle to another. In order to know the setting at which the  $dE/dx$  single-channel analyzer gates the 20-channel analyzer for the correct-energy alpha particles, a calibration curve was determined.

The alpha beam was scattered by an Au foil, and the scattered particles were observed at an angle of approximately  $30^\circ$ . The Au foil was chosen in order to reduce the number of reaction products in the scattered beam and to give a large counting rate. To simulate the change in energy of the alpha particles scattered into the detection head during the actual measurements, aluminum foils of various thicknesses were inserted into the path of the incident beam. As the foil thickness increased and the energy of the alpha beam decreased, the  $dE/dx$  pulse height increased and the  $E$  pulse height decreased. The center of the region on the  $dE/dx$  single-channel analyzer discriminator at which the 20-channel analyzer was gated for the various alpha-particle energies was recorded. A curve of this  $dE/dx$  pulse height vs the  $E$  pulse height was drawn and used during the actual scattering experiment to determine the correct setting of the single-channel analyzer.

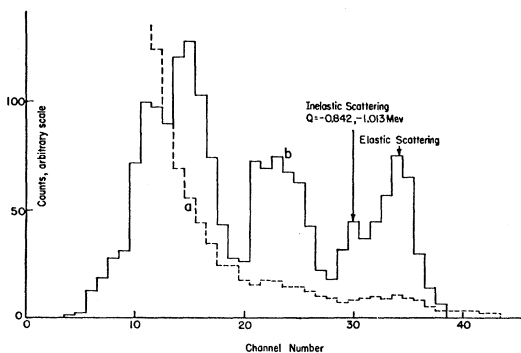


FIG. 3. Pulse-height distribution of particles observed at  $131^\circ$  with an Al target. *a*: analyzer not gated, mostly protons from  $(\alpha, p)$  reactions. *b*: analyzer gated for alpha particles. The ordinate scale for *b* is expanded by a factor  $\approx 10$ .



FIG. 4. Elastic scattering of 18.70-Mev alpha particles by Ag. The Rutherford cross section is given by  $\sigma(\Phi)_R = 35.1 \text{ csc}^4(\Phi/2) \text{ mb/sterad}$ .

### Multiple Scattering

In the calculation of the cross section it is assumed that the number of particles counted is proportional to the solid angle subtended by the defining aperture (see Fig. 2) at the target. In the actual measurement, however, a certain fraction of the particles entering the detection head in the proper direction will be lost because of multiple scattering in the window and the gas of the proportional counter. For a given geometry and given materials the loss depends on the alpha-particle energy only. Since the calculation of the correction appeared rather complicated, it was determined experimentally by counting the number of alpha particles scattered from a gold foil at a fixed angle with and without counter window and gas. The energy of the scattered particles was varied by reducing the beam energy with Al absorbers. With the  $A+CH_4$  filling, losses up to 30% were observed at the low alpha energies corresponding to backscattering from Al. For most of the measurements,  $He+CH_4$  was used as the counter gas.

## IV. RESULTS AND DISCUSSION

### Sample Scattering by Aluminum

Figure 3 is a sample of the energy spectrum of the particles observed at a laboratory angle of  $131^\circ$  with an Al target. Curve *a* shows the total spectrum, measured with the  $dE/dx$  selector inoperative; curve *b* exhibits the alpha-particle spectrum. No identification of the various peaks is made here, since it is only the highest, or elastic scattering, peak which is being studied. Some separation of elastic from inelastic scattering was necessary, however, and data on inelastic scattering obtained in this way are also presented.

### Elastic Scattering by Ag, Cu, and Al

Curves of  $\sigma(\Phi)/\sigma(\Phi)_R$  vs  $\Phi$  for elastic scattering from Ag, Cu, and Al are given in Figs. 4, 5, and 6. The alpha-

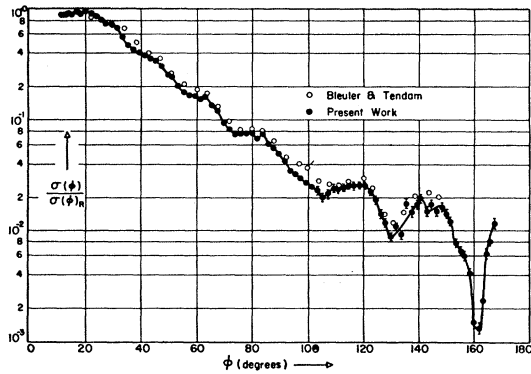


FIG. 5. Elastic scattering of 18.68-Mev alpha particles by Cu. The Rutherford cross section is given by  $\sigma(\Phi)_R = 14.1 \text{ csc}^4(\Phi/2)$  mb/sterad.

particle energies quoted are the laboratory energies at the center of the target. In general, measurements were taken in steps of  $2^\circ$ , but additional readings were taken near deep minima. The rms deviations of the accepted scattering angles, due to the finite solid angle and multiple scattering in the target, were  $0.4^\circ$  to  $0.5^\circ$  for Al, about  $0.75^\circ$  for Cu, and  $0.85^\circ$  for Ag. No resolution corrections were applied to the data since they were insignificant everywhere except at the deepest minima. There, they are small compared to the statistical error and the systematic error arising from the separation of the elastic and the inelastic groups. The latter may be as high as 20% at a few unfavorable angles, whereas the former were always kept below 5% and are negligible at most angles.

### Ag

The general trend of  $\sigma/\sigma_R$  is quite similar to that observed by Wall, Rees, and Ford<sup>4</sup> at  $E_\alpha = 21.2$  Mev. Our measurements extend to larger angles and (probably as expected) fail to show any strong structure or rise of the kind obtained from the semiclassical strong-absorption model. It is doubtful if the sharp minima shown in Fig. 4 should be considered as real; lack of time prevented a thorough check.

From the crossover criterion of Kerlee, Blair, and Farwell,<sup>9</sup> an interaction radius of  $9.4 \times 10^{-13}$  cm is calculated, in good agreement with the best-fit radii of  $9.38 \times 10^{-13}$  cm at 21.2 Mev<sup>4</sup> and  $9.26 \times 10^{-13}$  cm at 38.6 Mev<sup>10</sup> given in Blair's newest analysis.<sup>11</sup>

### Cu

For purpose of comparison the angular distribution obtained by Bleuler and Tendam<sup>2</sup> is also shown in Fig. 5. The agreement is very good, insofar as all small changes in slope as well as maxima and minima coincide. The extension to larger angles in the present work re-

vealed the very deep minimum at  $162^\circ$  whose explanation presumably will provide a rather stringent test for an accurate theory.

The crossover criterion would yield an interaction radius of  $9.0 \times 10^{-13}$  cm. If  $\sigma/\sigma_R$  is normalized to unity at small angles (the direct determination gave 0.90), the crossover radius is reduced to  $8.5 \times 10^{-13}$  cm which is still fairly large. On the other hand, Blair<sup>11</sup> found a best-fit radius of  $8.15 \times 10^{-13}$  cm for the old measurements; the crossover criterion probably becomes less reliable the more oscillatory the experimental distribution is.

### Al

Again, there is good agreement with the previous results. The present work shows deeper minima, as is to be expected because of the better angular resolution. The very narrow minimum near  $127^\circ$  had escaped de-

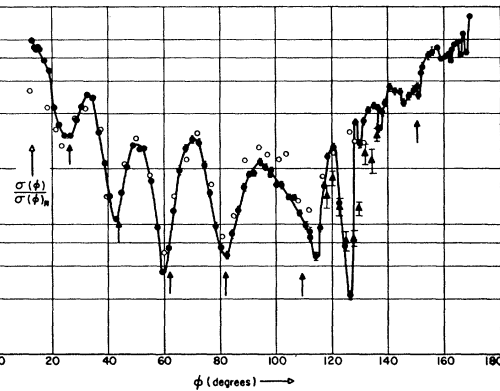


FIG. 6. Elastic scattering of alpha particles by Al. ● Present data, 18.82 Mev. The Rutherford cross section is given by  $\sigma(\Phi)_R = 3.27 \text{ csc}^4(\Phi/2)$  mb/sterad. ○ Bleuler and Tendam,<sup>2</sup> 18.95 Mev. ▲ Control measurements with plates, 19.52 Mev. The arrows indicate the zeros of  $j_1(qR)$  for  $R = 6.41 \times 10^{-13}$  cm.

tection in the original measurements. It was checked independently with the aid of photographic plates positioned behind an array of slits every  $2.5^\circ$ . The results confirm the existence of the minimum. Between the two runs, the cyclotron had been reshimmed and the beam energy was increased. It is probable that the difference in the width of the minima is due to this energy shift.

There is a striking contrast between the back-angle distribution ( $\Phi > 130^\circ$ ) for Al and the distributions observed by Seidlitz *et al.*<sup>1</sup> for Ne and A. The latter exhibited pronounced minima and maxima whereas the present Al curve shows essentially only a general rise. Some of the rapid fluctuations indicated in Fig. 6 are undoubtedly spurious.

An interaction radius may be calculated by assuming the approximate validity of the Born-approximation formula for scattering from a square-well potential and identifying the minima with the zeros of  $j_1(qR)$

<sup>9</sup> Kerlee, Blair, and Farwell, *Phys. Rev.* **107**, 1343 (1957).

<sup>10</sup> Igo, Wegner, and Eisberg, *Phys. Rev.* **101**, 1508 (1956).

<sup>11</sup> J. S. Blair, *Phys. Rev.* **108**, 827 (1957).

$=j_1(2kR \sin(\Phi/2))$ ,<sup>12</sup> where  $k$  is the wave number of the system. The resulting value of  $6.4 \times 10^{-13}$  cm is appreciably larger than the value ( $5.4 \times 10^{-13}$  cm) found by Igo *et al.*<sup>10</sup> at 40 Mev, but agrees with the general trend at 18–19 Mev observed by Seidlitz *et al.*

### Inelastic Scattering

The inelastic peaks observed do not correspond to single alpha-particle groups. For Al, the groups from transitions to the first two excited states at 0.842 and 1.013 Mev are not resolved. The inelastic peak for Cu is due to at least four transitions, i.e., those to the two lowest levels in each isotope.

Figures 7 and 8 show the angular distributions observed for Al and Cu. In both cases, the elastic peak is so much larger in the forward direction that the inelastic peak could not be measured with any reliability. As in the case of the elastic scattering, some of the rapid

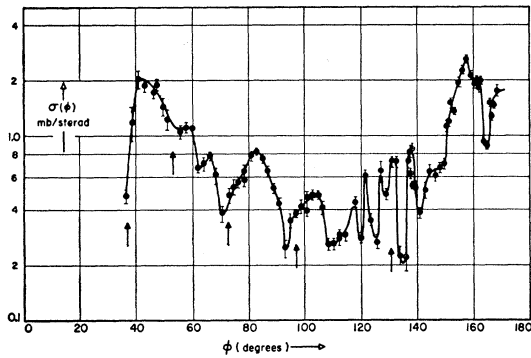


FIG. 7. Inelastic scattering of 18.82-Mev alpha particles by Al;  $Q = -0.842$  and  $-1.013$  Mev. The arrows indicate the zeros of  $j_2(qR)$  for  $R = 6.41 \times 10^{-13}$  cm.

fluctuations at large angles are doubtful; the curves are shown chiefly to illustrate the general trend.

The angular distribution for Al is much less regular than that found for Ne, A,<sup>1</sup> and Mg.<sup>12,13</sup> The same difference was observed for elastic scattering; it is probably due to the fact that Al has odd  $Z$ . In view of the success of direct-interaction theories for Ne, Mg, and

<sup>12</sup> P. C. Gugelot and M. Rickey, Phys. Rev. **101**, 1613 (1956).

<sup>13</sup> H. J. Watters, Phys. Rev. **103**, 1763 (1956).

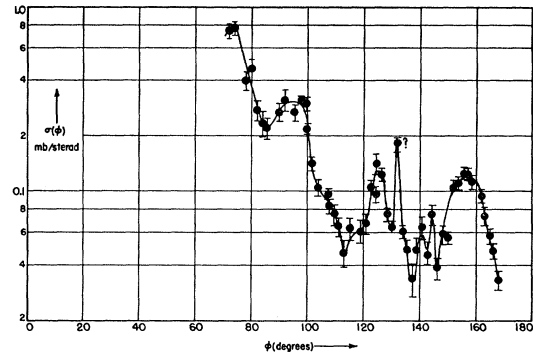


FIG. 8. Inelastic scattering of 18.68-Mev alpha particles by Cu;  $Q = -0.67$  to  $-1.14$  ( $-1.7?$ ) Mev.

A, one may try to apply them to Al. The spin of the ground state is  $\frac{5}{2}$ , with negative parity, whereas the excited states are  $\frac{1}{2}^-$  and  $\frac{3}{2}^-$ . The chief contribution to both transitions would have an angular dependence of the type  $[j_2(qR)]^2$  where  $q$  is the magnitude of the difference between initial and final wave vector. The arrows shown in Fig. 7 indicate the zeros of this function for a radius of  $R = 6.41 \times 10^{-13}$  cm. There appears to be a fair correlation with the minima of the distribution. For the transition to the second excited state there could also be a contribution involving  $j_4(qR)$  since a vectorial spin change of 4 units ( $\frac{5}{2}^- \rightarrow \frac{3}{2}^-$ ) is possible. No attempt has been made to include this or to use the more elaborate formulas given by Butler,<sup>14</sup> since the groups corresponding to the two levels were not separated.

### ACKNOWLEDGMENTS

The authors wish to express their appreciation to Dr. J. W. Blue for his advice on the design of many of the electronic circuits, and to Dr. L. Seidlitz for the design of the scattering chamber and its remote controls. Acknowledgement is also made to Mr. F. Hobaugh and to Mr. E. L. Robinson for the many hours of cyclotron bombardments, to Mr. J. Moore and Mr. G. Lawler for their advice and help with the modifications of the scattering chamber, and to Mr. J. C. Corelli for his invaluable aid during the measurements and calculations.

<sup>14</sup> S. T. Butler, Phys. Rev. **106**, 272 (1957).